Vietnam Journal of Mechanics, VAST, Vol. 29, No. 3 (2007), pp. 303 - 319
Special Issue Dedicated to the Memory of Prof. Nguyen Van Dao

MODELING AND STABILITY ANALYSIS FOR AN ULTRASONIC MOTOR

STEFANIE GUTSCHMIDT, GOTTFRIED SPELSBERG-KORSPETER, PETER HAGEDORN

Department of Mechanical Engineering,
Dynamics and Vibrations Group
Technische Universitt Darmstadt,
Hochschulstr. 1, 64289 Darmstadt, Germany

Abstract. The development of motor models, adequate for motor design and optimization is still behind the technological state of the art. The reason for this lies in the fact that a couple of years ago the main emphasis regarding ultrasonic motors was on finding new principles or prototypes while today this has shifted towards optimization of known working concepts and motors. A systematic motor optimization demands, among other things, a detailed dynamical understanding of the motor which not too often exists for ultrasonic motors in general.

The present study deals with modeling a wobbling disk piezoelectric motor. For the model the analytic steady state solution is derived and stability of the solution is investigated. The model and the analytic steady state solution yield a detailed insight in essential dynamical phenomena by which the motor is driven. The model framework may be a guideline providing understanding in the working principle, dynamics, weighting of the parameters with respect to reliable, stable operation and optimization of such motors.
Keywords: wobbling disk, ultrasonic motor, nonlinear dynamics, stability.

1. INTRODUCTION

In this paper we derive a model for a wobbling disk ultrasonic motor (USM) considering as example CANON's bar-type motor (Fig. 1). This motor was the first mass produced

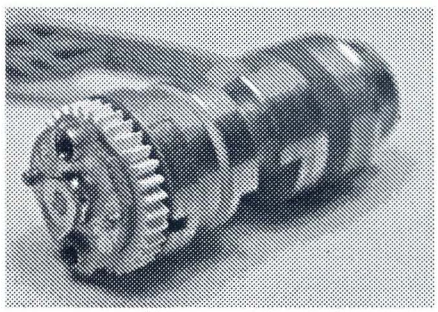

Fig. 1. Photograph of CANON's bar-type ultrasonic motor U400

USM in the world and has been used in Canon's autofocus lenses for more than 16 years now. The design of ultrasonic motors has so far mainly been an empirical process based on experiments and testing. Design of the parts is done using commercial FE-packages analyzing the vibrational behavior. However it is rather difficult to choose the parameters for such models properly. Mathematical models such as the one presented in this paper are useful to understand the dynamical phenomena and help to identify crucial parameters that determine the behavior of the motor. Such models may help to optimize the motor design in early development stages and avoid some testing. Today mathematical models exist for traveling wave ultrasonic motors, [1, 2]. A mathematical model for a wobbling disk USM is introduced in this paper in which the stability analysis of the steady state solution is chosen to be in the center of the studies. Stability investigations are essential to justify the model and a certain robustness of the motor behavior.

Design and Working Principle

An exploded view of the motor is shown in Fig. 2. The major components are the piezoceramic, the rotor and the stator.

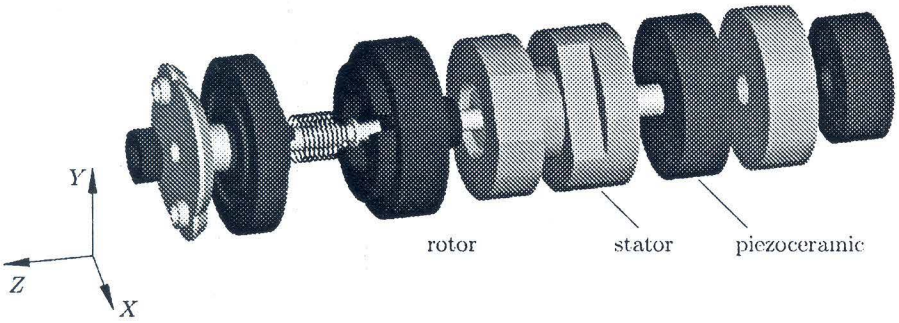

Fig. 2. Exploded view of the motor

A detailed explanation of the design and working principle of CANON's bar-type USM can be found in [3] or [4]. In the piezoceramic two bending modes of the stator are excited. The excitation frequency is chosen near the eigenfrequency of the stator corresponding to the first bending mode. The two bending modes are mutually perpendicular, so that a circulating bending mode is generated (Fig. 3). The contact point on the stator's surface

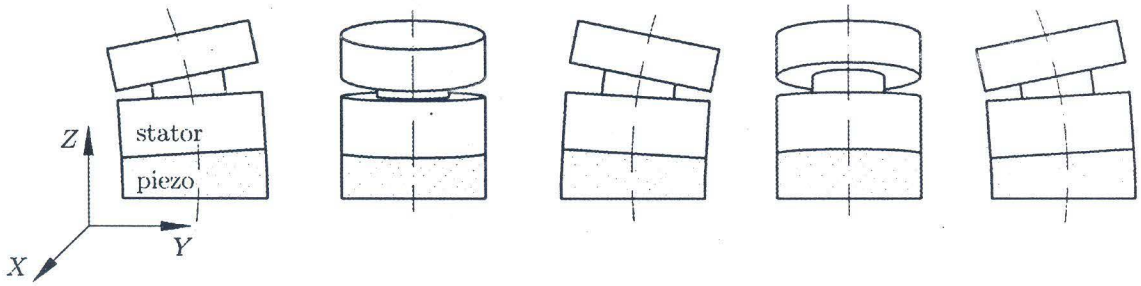

Fig. 3. Bending vibrations of the stator

then describes a circular trajectory. The rotor is pressed onto the stator by a spring such that there is frictional contact between the highest point of the stator and the rotor for all times. The rotor is driven by the torque of the frictional contact force between rotor and stator.

2. MODELING

Experiments and FE analysis have shown that the lower part of the stator is almost at rest (cf. Fig. 3). Therefore, it is reasonable to model only the upper part of the stator considering rotor and stator as rigid bodies. The stator is given the degrees of freedom (DOF) as shown in Fig. 4. A tilting of the stator against the $X - Y$ plane is restrained

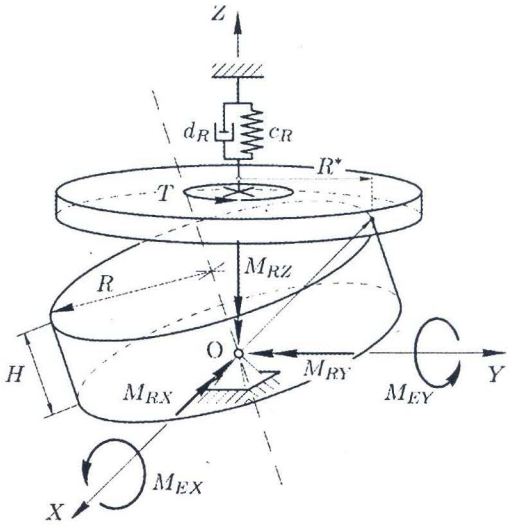

Fig. 4. Schematic drawing of the model

by a restoring torque proportional to the tilting angle. Restoring and damping torque can be modeled as infinitesimal spring-damper elements distributed about the $X - Y$ plane. The excitation of the stator is modeled as a torque rotating in the $X - Y$ plane with the angular velocity Ω.

The rotor can move freely in the Z-direction and rotate about the Z-axis as pictured in Fig. 4. The rotor is pressed onto the stator by a spring. Movement in direction of the Z-axis is damped proportional to the velocity. We assume that the spring is stiff enough and that there is enough preload such that rotor and stator are in contact at all times. In the following we assume that between rotor and stator no slip occurs.

Kinematics

The position of the stator can be fully described by the EULER angles ϕ, θ, ψ that are defined in Fig. 5.

In the remainder the reference frames defined in Table 1 are frequently used.

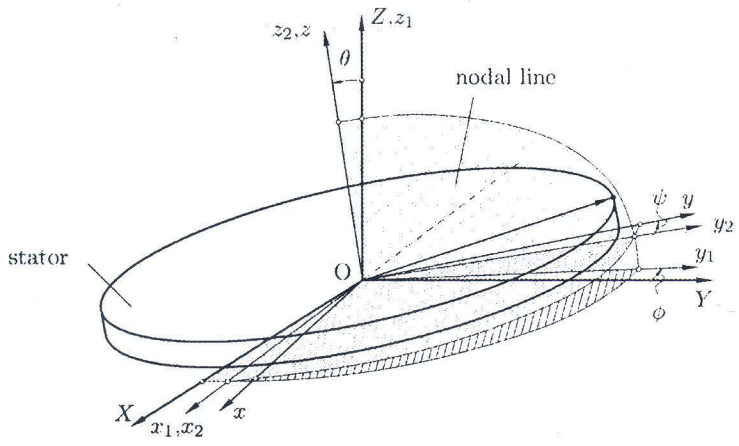

Fig. 5. Reference frames; EULER angles

Table 1. Reference frames

	coordinates	name	rotation
N	X, Y, Z	inertial frame	
A	x_1, y_1, z_1	auxiliary frame	ϕ about Z
B	x_2, y_2, z_2	auxiliary frame	θ about x_1
K	x, y, z	body-fixed frame	ψ about z_2

Table 2. Forces and torques

	forces/torques	components in N
F_R	restoring force	
F_D	damping force	
$\vec{F}_c$	contact force	F_r, F_t, F_n
$\vec{M}_R$	restoring torques	M_{KX}, M_{KY}, M_{KZ}
$\vec{M}_D$	damping torques	M_{DX}, M_{DY}, M_{DZ}
$\vec{M}_E$	excitation torque	M_{EX}, M_{EY}, M_{EZ}
T	loading torque	

Dynamics and equations of motion

The freebody diagram of the motor is depicted in Fig. 6. In the following we derive the equations of motion for the rotor and stator. Forces and torques (listed in Table 2) are modeled based on previous assumptions. The detailed mathematical expressions for the force and torque vectors are explained as we go along.

Formulating the principle of linear momentum of the rigid body of the rotor in the Z-direction yields:

$$M\ddot{Z} = F_n - F_R - F_D \qquad \text{with} \qquad F_R = F_0 + c_R Z, \quad F_D = d_R \dot{Z}, \tag{2.1}$$

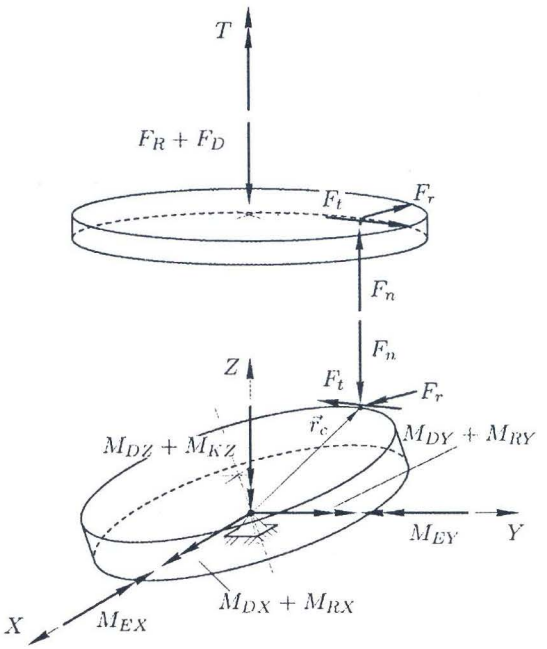

Fig. 6. Freebody diagram

where M, c_R, d_R, Z and $\dot{Z}$ are the mass, the stiffness coefficient, the damping coefficient, the axial coordinate and the time derivative of the coordinate in axial direction of the rotor, respectively. F_0 is the preload. From the balance of moment of momentum about the Z-axis follows:

$$I_R \ddot{\phi}_R = F_t R^* - T. \tag{2.2}$$

$R^* = R\cos\theta - H\sin\theta$ is the contact radius, I_R and ϕ_R are the moment of inertia and the angular coordinate about the inertial Z-axis of the rotor, respectively. The kinematic restrictions for permanent contact between rotor and stator are formulated as

$$Z = \vec{r}_c \cdot \vec{e}_Z. \tag{2.3}$$

From the stick condition, i.e. that the velocities of the contact point on the rotor's surface and on the stator's surface are equal, follows

$$\dot{\phi}_R = -\frac{(\vec{\omega} \times \vec{r}_c) \cdot \vec{e}_{x_1}}{R^*}, \tag{2.4}$$

where $\vec{\omega}$ is the angular velocity of the stator. Neglecting F_r, the vector of the contact force $\vec{F}_c$ expressed in frame A is

$$\vec{F}_c = -F_t \vec{e}_{x_1} - F_n \vec{e}_{z_1}. \tag{2.5}$$

The equations of motion for the rotor modeled with 2 DOF are given by (2.1) and (2.2) can completely be expressed in terms of EULER angles. These equations can be solved for the components of the contact force.

In the body-fixed frame K the equations of motion of the stator simplify to EULER's equations:

$$\frac{d}{dt}\vec{L}^{(\mathrm{O})} = \begin{bmatrix} I_{xx}\dot{\omega}_x - (I_{yy} - I_{zz})\omega_y\omega_z \\ I_{yy}\dot{\omega}_y - (I_{zz} - I_{xx})\omega_z\omega_x \\ I_{zz}\dot{\omega}_z - (I_{xx} - I_{yy})\omega_x\omega_y \end{bmatrix}^K = \vec{M}^{(\mathrm{O})}, \tag{2.6}$$

where I_{ii}, $\forall i \in \{x, y, z\}$ are the entries of the matrix of the moment of inertia and $\vec{M}^{(o)}$ is the torque vector given by

$$\vec{M}^{(\mathrm{O})} = \vec{M}_E - \vec{M}_R - \vec{M}_D + \vec{r}_c \times \vec{F}_c. \tag{2.7}$$

In the following, the torque vector shall be discussed in detail. The excitation torque created by the piezo element $\vec{M}_E$ is modeled by a vector rotating in the $X - Y$ plane having an amplitude m_0

$$\vec{M}_E = m_0 \cos \Omega t \; \vec{e}_X + m_0 \sin \Omega t \; \vec{e}_Y. \tag{2.8}$$

The restoring and damping torques are depicted in Fig. 7.

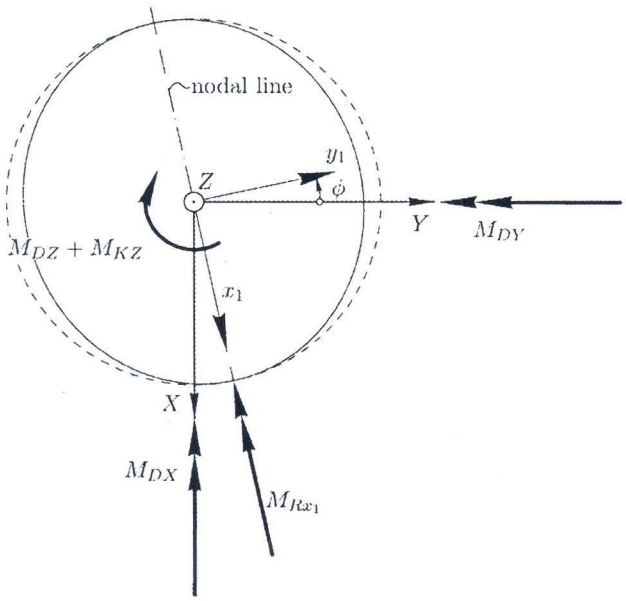

Fig. 7. Definition of restoring and damping torques

The restoring torque is assumed to be proportional to the tilting angle between the $x - y$ and the $X - Y$ plane and can be defined as $M_{Rx_1} = c_r\theta$ about the nodal line, so that the restoring torque is

$$\vec{M}_R = c_r\theta \; \vec{e}_{x_1} + c_t \left[\phi + \psi \cos\theta\right] \vec{e}_Z. \tag{2.9}$$

The second part in (2.9) is a torque proportional to the twisting of the stator about the Z-axis, where $\phi + \psi \cos\theta$ is the expression of the twisting angle. According to the phenomenological description (Section 1) the damping torque is given by

$$\vec{M}_D = d_r\omega_X \; \vec{e}_X + d_r\omega_Y \; \vec{e}_Y + d_t\omega_Z \; \vec{e}_Z \,, \tag{2.10}$$

i.e. a damping torque that is proportional to the angular velocity components of the stator. The moment of the contact force is defined as

$$\vec{M}_C = \vec{r}_c \times \vec{F}_c \,. \tag{2.11}$$

3. STATIONARY SOLUTION

At the end of start-up the rotor will not perform any vibrations in Z-direction or about the Z-axis, which yields: $\dot{Z} = 0$, $\ddot{Z} = 0$, $\dot{\theta} = 0$, $\ddot{\theta} = 0$ and $\omega_Z = \dot{\phi} + \dot{\psi}\cos\theta = 0$. By substitution of these in (2.6) the stationary solution takes the form

$$\bar{\phi}(t) = \Omega\, t + \alpha, \tag{3.1a}$$

$$\bar{\theta} = \text{const}, \tag{3.1b}$$

$$\bar{\psi}(t) = -\frac{\Omega\, t}{\cos\bar{\theta}} + \beta. \tag{3.1c}$$

The angles α and β are phase angles relative to the excitation. Substitution of this ansatz into (2.6) yields an equation of the form

$$\frac{d}{dt}\overline{\vec{L}} = \overline{\vec{M}}_E - \overline{\vec{M}}_D - \overline{\vec{M}}_R + \overline{\vec{M}}_C. \tag{3.2}$$

Overlined variables denote variables in steady state operation. The expressions in (2.6) are lengthy in general. However, the equations for the X-direction and Y-direction, respectively are linearly dependent since they only differ by a phase angle of $\pi/2$. If a $\bar{\theta}$ can be found such that the equation for the X-direction is valid for all times it can be shown, that $\bar{\phi} = \Omega\, t + \alpha$ satisfies (2.6).

Time is eliminated from (2.6) by summing the equation for the X-direction and the imaginary unit times the equation for the Y-direction using

$$\cos(\Omega\, t + \alpha) + i\sin(\Omega\, t + \alpha) = \mathrm{e}^{i\,\Omega\, t}(\cos\alpha + i\,\sin\alpha), \tag{3.3}$$

yielding an equation of the form

$$f_1(\alpha, \bar{\theta}) + i\, f_2(\alpha, \bar{\theta}) = 0. \tag{3.4}$$

In order to satisfy (3.4), $f_1(\alpha, \bar{\theta})$ and $f_2(\alpha, \bar{\theta})$ have to vanish, i.e.

$$f_1(\alpha, \bar{\theta}) = 0\,, \tag{3.5a}$$

$$f_2(\alpha, \bar{\theta}) = 0\,. \tag{3.5b}$$

Equations (3.5a) and (3.5b) can be solved numerically. For the given set of parameters (Appendix A) the tilting angle takes the value $\bar{\theta} = 0.81836 \cdot 10^{-4}$ with the corresponding phase angle $\alpha = 5.16$ degrees. From the equation in Z-direction of (2.6) follows

$$\beta = \frac{1}{c_t \cos\bar{\theta}}\,(T + c_t\,\alpha) \tag{3.6}$$

and hence $\beta = -1.98$ degrees. We emphasize however that not for all parameters a physically reasonable solution to (3.5a) and (3.5b) can be found.

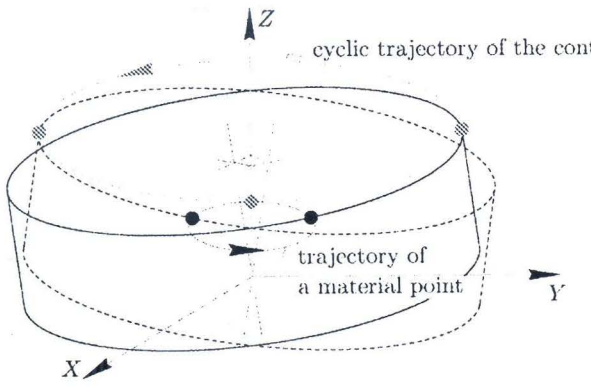

Fig. 8. Kinematics of an arbitrary surface point of the stator

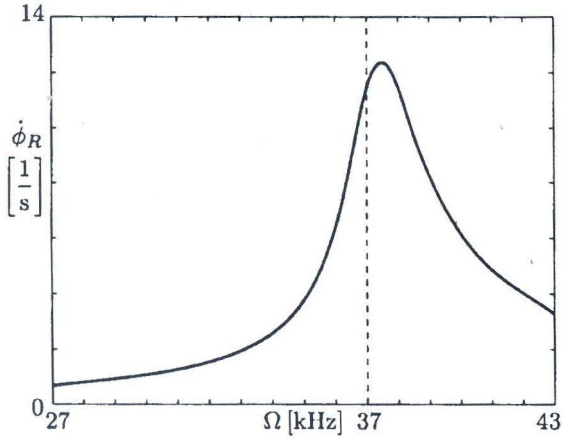

Fig. 9. Characteristic excitation frequency

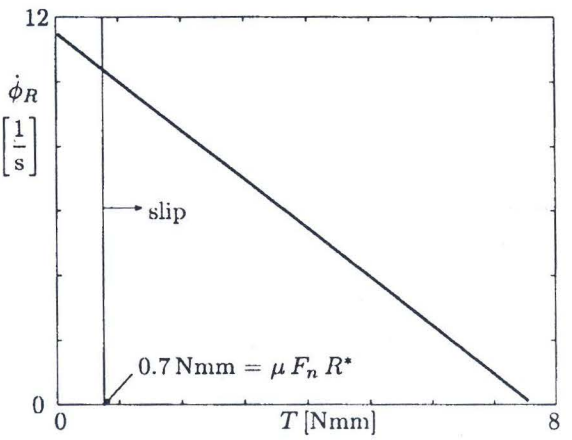

Fig. 10. Characteristic load

Discussion of the Stationary Solution

The steady state solution is illustrated in Fig. 8. The contact point of the stator moves on a circular orbit. Any arbitrary surface point of the stator moves on an elliptical trajectory. Note that the directions of motion of the contact point and the rotor are opposite. This becomes obvious following the motion at the instant where the surface point is the contact point at the same time (cf. Fig. 8).

Linearization of (2.4) for small angles $\bar{\theta}$ yields an approximate formula for the rotational speed of the rotor

$$\dot{\phi}_R = \frac{H\bar{\theta}}{R}\Omega. \tag{3.7}$$

Since $\bar{\theta}$ is small, $\dot{\phi}_R$ is much smaller than the excitation frequency Ω. This is a typical feature for ultrasonic motors which makes the use of additional gears unnecessary in many applications. This reduces noise effects and simplifies controllability of the motor. One qualitatively recognizes from (3.7) that the angular velocity of the motor depends on the

excitation frequency and the angle $\bar{\theta}$ which is a function of Ω, m_0 and T and the geometrical parameters.

Having found the steady state solution one immediately has the characteristics of the motor, too [4,5]. The most important ones are shown in Figs. 9, 10 and 11.

It is seen that the angular velocity has a maximum near an eigenfrequency of the stator at 36.8 kHz (c.f. Fig. 9). From Fig. 10 it is seen that the angular velocity of the rotor decreases with increasing load. Above a load of 9.7 Nmm slip will occur between rotor and stator. In agreement with (3.7) an increase of the driving torque will increase the tilting angle θ and therefore speed up the rotor.

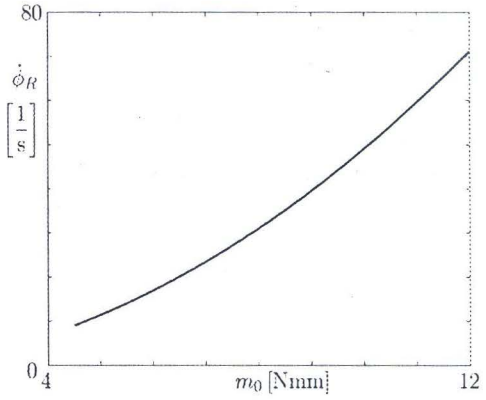

Fig. 11. Characteristic excitation torque

The steady state solution is also verified by the transient solution of the equations of motion that has been done in [4,5].

4. STABILITY ANALYSIS

In the following we investigate the stability of the steady state solution previously found. For the stability analysis we use the stability definition of LIAPUNOV, [6]. A comprehensive stability analysis including parameter variations was done in [5].

First approximation method for linear differential equations with periodic coefficients

For differential equations with periodic coefficients of the form

$$\dot{\mathbf{x}} = \mathbf{f}(\mathbf{x}, t) \tag{4.1}$$

with $\mathbf{f}(\mathbf{x}, t) = \mathbf{f}(\mathbf{x}, t + T)$, stability of the solution $\mathbf{x} = \mathbf{0}$ is determined by the linearized differential equation provided that certain conditions hold, [7]. Expansion of $\mathbf{f}(\mathbf{x}, t)$ about $\mathbf{x} = \mathbf{0}$ yields

$$\begin{aligned} \dot{\mathbf{x}} &= \mathbf{A}(t)\,\mathbf{x} + \mathbf{h}(\mathbf{x}, t)\,, \\ \mathbf{A}(t) &= \mathbf{A}(t + T)\,. \end{aligned} \tag{4.2}$$

If $\mathbf{h}(\mathbf{x}, t)$ is continuous and if there exists a domain such that $t \geq t_0$ and $|x_i| < H$, in which for a sufficiently small constant C

$$\|\mathbf{h}(\mathbf{x}, t)\|_\infty \leq C(|x_1| + \ldots + |x_n|) = C\|\mathbf{x}\|_1 \tag{4.3}$$

holds, one can conclude stability or instability from the first approximation

$$\dot{\mathbf{x}} = \mathbf{A}(t)\,\mathbf{x}\,, \qquad \mathbf{A}(t) = \mathbf{A}(t+T)\,. \tag{4.4}$$

Equation (4.4) is a linear differential equation with periodic coefficients.

Let $\mathbf{\Phi}(t) = [\mathbf{x_1}(t), ..., \mathbf{x_n}(t)]$ be a system of fundamental solutions of (4.4). From the theory of linear differential equations one has

$$\mathbf{\Phi}(t+T) = \mathbf{B}\mathbf{\Phi}(t)\,,$$

where $\mathbf{B}$ is a constant matrix. The equation

$$|\mathbf{B} - \lambda\mathbf{E}| = 0 \tag{4.5}$$

is called characteristic equation of (4.4). It has been shown that the characteristic equation is independent of the choice of a fundamental system [7]. Corresponding to every eigenvalue of (4.5) there is a particular solution of the form

$$\mathbf{x} = e^{\alpha_k t}\widetilde{\mathbf{f}}(t)\,, \qquad \alpha_k = \frac{1}{T}\ln\lambda_k\,, \qquad \widetilde{\mathbf{f}}(t) = \widetilde{\mathbf{f}}(t+T)\,.$$

For stability of the solution $\mathbf{x} = \mathbf{0}$ of (4.4) the following theorem holds:

Theorem: *([7]) If for every eigenvalue λ_k of the characteristic equation of (4.4) $|\lambda_k| < 1\,\forall\,k$ holds, and if the conditions for $\mathbf{h}(\mathbf{x}, t)$ are satisfied, then the solution $\mathbf{x} = \mathbf{0}$ of (4.1) is asymptotically stable in the sense of* LIAPUNOV. *If $|\lambda_k| > 1$ for any k, then the solution $\mathbf{x} = \mathbf{0}$ of (4.1) is unstable. For the remaining case stability is determined by the nonlinear term $\mathbf{h}(\mathbf{x}, t)$.*

Stability analysis of the stationary solution

For the analysis of stability we use the first order system of the equations of motion (2.6)

$$\mathbf{M}(\mathbf{x})\dot{\mathbf{x}} = \mathbf{f}(\mathbf{x}, t) \tag{4.6}$$

where $\mathbf{x} = [\phi, \theta, \psi, \dot{\phi}, \dot{\theta}, \dot{\psi}]^T$. Substituting $\mathbf{x} = \overline{\mathbf{x}} + \triangle\mathbf{x}$ in (4.6) yields $\mathbf{M}(\overline{\mathbf{x}}+\triangle\mathbf{x})[\dot{\overline{\mathbf{x}}}+\triangle\dot{\mathbf{x}}] = \mathbf{f}(\overline{\mathbf{x}}+\triangle\mathbf{x}, t)$. The stability analysis of the solution $\overline{\mathbf{x}}$ can therefore be done by investigating the stability of $\triangle\mathbf{x} = 0$ and can be performed as described in the previours paragraph. Equations (4.6) and (4.1) differ by the mass matrix $\mathbf{M}$ on the left hand side of (4.6). This is equivalent to

$$\dot{\overline{\mathbf{x}}} + \triangle\dot{\mathbf{x}} = \mathbf{M}^{-1}(\overline{\mathbf{x}} + \triangle\mathbf{x})\mathbf{f}(\overline{\mathbf{x}} + \triangle\mathbf{x}, t) = \widetilde{\mathbf{f}}(\overline{\mathbf{x}} + \triangle\mathbf{x}, t)\,, \tag{4.7}$$

since $\mathbf{M}$ is invertible. One now expands $\widetilde{\mathbf{f}}(\overline{\mathbf{x}}+\triangle\mathbf{x}, t)$ about $\overline{\mathbf{x}}$ which, because of $\dot{\overline{\mathbf{x}}} = \widetilde{\mathbf{f}}(\overline{\mathbf{x}}, t)$, yields

$$\triangle\dot{\mathbf{x}} = \mathbf{A}(t)\triangle\mathbf{x} + \mathbf{h}(\triangle\mathbf{x}, t)\,, \tag{4.8}$$

which is an equation of the form (4.2), where

$$a_{ij} = \frac{\partial}{\partial x_j} \widetilde{f}_i(\overline{\mathbf{x}}, t)\,,$$
$$h_i = \frac{\partial^2}{\partial x_j \partial x_k} \widetilde{f}_i(\xi, t) \triangle x_j \triangle x_k\,, \quad \xi \in [0, \triangle \mathbf{x}].$$

The matrix $\mathbf{A}$ is JACOBI matrix of $\widetilde{\mathbf{f}}$, and $\mathbf{h}$ is a vector of higher order terms. The linearly increasing and decreasing components $\overline{x}_1$ and $\overline{x}_3$ appear in the arguments of trigonometric functions sin and cos. Other components of $\overline{\mathbf{x}}$ are constant, hence $\mathbf{A}$ is periodic. Stability analysis can now be performed as described in the previous section. The inversion of $\mathbf{M}$ is computationally expensive and makes the calculation of the JACOBlan much more complicated.

A different approach is to expand both sides of (4.6) directly. An equation of the form

$$\begin{aligned} \mathbf{M}(t) \triangle \dot{\mathbf{x}} &= \mathbf{A}(t) \triangle \mathbf{x} + \mathbf{h}(\triangle \mathbf{x}, \triangle \dot{\mathbf{x}}, t)\,, \\ \mathbf{M}(t) &= \mathbf{M}(t+T)\,, \\ \mathbf{A}(t) &= \mathbf{A}(t+T)\,. \end{aligned} \tag{4.9}$$

is obtained. Note that now $\mathbf{h}$ is also depending upon $\triangle \dot{\mathbf{x}}$. Since $\mathbf{M}$ is invertible, the steps of the approach described in the previours section remain the same. The only difference is that (4.3) is now written as

$$\|\mathbf{M}(t)^{-1} \mathbf{h}(\triangle \mathbf{x}, \triangle \dot{\mathbf{x}}, t)\|_\infty < C(|\triangle x_1| + \ldots + |\triangle x_n|) = C \|\triangle \mathbf{x}\|_1\,, \tag{4.10}$$

where C is again a sufficiently small constant. For convenience in the following we use the cartesian index notation applying EINSTEIN's summation convention. Equation (4.6) is then written as

$$m_{ij}(\overline{\mathbf{x}} + \triangle \mathbf{x})[\dot{\overline{x}}_j + \triangle \dot{x}_j] = f_i(\overline{\mathbf{x}} + \triangle \mathbf{x}, t)\,. \tag{4.11}$$

We linearize (4.10) and show that the linear system fulfills the criteria mentioned in the previours section guaranteeing that stability of (4.6) depends on the linear system only, [5]. We expand m_{ij} and f_i about $\triangle \mathbf{x} = \mathbf{0}$ and get

$$m_{ij}(\overline{\mathbf{x}} + \triangle \mathbf{x}) = m_{ij}(\overline{\mathbf{x}}) + \frac{\partial}{\partial x_k} m_{ij}(\overline{\mathbf{x}}) \triangle x_k + T_{ij}^{H_1}\,, \tag{4.12a}$$

$$f_i(\overline{\mathbf{x}} + \triangle \mathbf{x}, t) = f_i(\overline{\mathbf{x}}, t) + \frac{\partial}{\partial x_k} f_i(\overline{\mathbf{x}}, t) \triangle x_k + T_i^{H_2}\,. \tag{4.12b}$$

Since

$$\mathbf{M} = \begin{bmatrix} 1 & 0 & 0 & \ldots & \ldots & 0 \\ 0 & 1 & 0 & \ldots & \ldots & 0 \\ 0 & 0 & 1 & \ldots & \ldots & 0 \\ \vdots & \ldots & \ldots & m_{44}(\bar{x}_1, \bar{x}_2, \bar{x}_3) & m_{45}(\bar{x}_1, \bar{x}_2, \bar{x}_3) & m_{46}(\bar{x}_1, \bar{x}_2, \bar{x}_3) \\ \vdots & \ldots & \ldots & m_{54}(\bar{x}_1, \bar{x}_2, \bar{x}_3) & m_{55}(\bar{x}_1, \bar{x}_2, \bar{x}_3) & m_{56}(\bar{x}_1, \bar{x}_2, \bar{x}_3) \\ 0 & \ldots & \ldots & m_{64}(\bar{x}_1, \bar{x}_2, \bar{x}_3) & m_{65}(\bar{x}_1, \bar{x}_2, \bar{x}_3) & m_{66}(\bar{x}_1, \bar{x}_2, \bar{x}_3) \end{bmatrix}$$

and $\dot{\overline{\mathbf{x}}} = [\Omega,\, 0,\, -\dfrac{\Omega}{\cos\theta}, 0, 0, 0]^T$ we have $\dfrac{\partial}{\partial x_k} m_{ij}(\overline{\mathbf{x}}) \triangle x_k \dot{\overline{x}}_i = 0$. $m_{ij}(\overline{\mathbf{x}})\dot{\overline{x}}_i = f_i(\overline{\mathbf{x}}, t)$ yields

$$m_{ij}(\overline{\mathbf{x}}) \triangle \dot{x}_j = \frac{\partial}{\partial x_k} f_i(\overline{\mathbf{x}}, t) \triangle x_k + h_i(\triangle \mathbf{x}, \triangle \dot{\mathbf{x}}, t)\,, \tag{4.13a}$$

where

$$h_i(\triangle \mathbf{x}, \triangle \dot{\mathbf{x}}, t) = T_i^{H_2} - T_{ij}^{H_1}(\dot{\overline{x}}_j + \triangle \dot{x}_j) - \frac{\partial}{\partial x_k} m_{ij}(\overline{\mathbf{x}}) \triangle x_k \triangle \dot{x}_j\,. \tag{4.13b}$$

Showing that (4.13b) meets the criteria for stability by first approximation we note that all terms in (4.13b) are continuous, since $\mathbf{M}(\mathbf{x}, t)$ and $\mathbf{f}(\mathbf{x}, t)$ are arbitrarily often differentiable. It remains to be shown that (4.10) holds. Hence, we first note that since (4.3) holds in a domain around zero it follows from (4.8) that $\|\triangle \dot{\mathbf{x}}\|_\infty < \infty$ for $\|\triangle \mathbf{x}\|_\infty < H$ since $\mathbf{M}$ and $\mathbf{f}$ are periodic with respect to T and bounded. Furthermore, $\mathbf{M}$ is invertible. The higher order terms from (4.12a) and (4.12b) are given by

$$\begin{aligned} T_{ij}^{H_1} =& \triangle x_k \frac{\partial^2}{\partial x_k \partial x_l} m_{ij}(\xi, t) \triangle x_l \quad \xi \in [0, \triangle \mathbf{x}]\,, \\ T_i^{H_2} =& \triangle x_k \frac{\partial^2}{\partial x_k \partial x_l} f_i(\eta, t) \triangle x_l \quad \eta \in [0, \triangle \mathbf{x}]\,. \end{aligned}$$

The entries m_{ij} and f_i are bounded periodic functions. Therefore

$$\begin{aligned} \frac{\partial^2}{\partial x_k \partial x_j} f_i(\eta, t) \leq& C_{ijk}^1 \quad \eta \in [0, \triangle \mathbf{x}] \wedge \forall t \geq t_0\,, \\ \frac{\partial^2}{\partial x_k \partial x_l} m_{ij}(\xi, t) \leq& C_{ijkl}^2 \quad \xi \in [0, \triangle \mathbf{x}] \wedge \forall t \geq t_0\,, \\ \frac{\partial}{\partial x_k} m_{ij}(\overline{\mathbf{x}}) <& C_{ijk}^3 \quad \forall t \geq t_0\,, \end{aligned}$$

where C_{ijk}^n are real constants with $C_{ijk}^n < \infty$. There is a domain $\|\triangle \mathbf{x}\|_\infty < H$, in which

$$h_i(\triangle \mathbf{x}, \triangle \dot{\mathbf{x}}, t) \leq C_{ijk}^1 \triangle x_j \triangle x_k + C_{ijkl}^2 \triangle x_k \triangle x_l (\dot{\overline{x}}_j + \triangle \dot{x}_j) + C_{ijk}^3 \triangle x_k \triangle \dot{x}_j$$

holds. Since $\dot{\overline{x}}_j + \triangle \dot{x}_j$ is bounded it follows

$$h_i(\triangle \mathbf{x}, \triangle \dot{\mathbf{x}}, t) \leq C_{ijk}^4 \triangle x_j \triangle x_k + C_{ijk}^3 \triangle x_j \triangle \dot{x}_k\,.$$

The elements $m_{ij}(\overline{\mathbf{x}})$ are periodic with respect to T and bounded, therefore this also holds for the m_{ij}^{-1}, where m_{ij}^{-1} are the entries of the inverse of $\mathbf{M}(\overline{\mathbf{x}}) = \mathbf{M}(t) = m_{ij}(\overline{\mathbf{x}})$. It follows that there exists a domain Q with $\|\triangle \mathbf{x}\|_\infty < H$ in which

$$m_{ij}^{-1}(t) h_j(\triangle \mathbf{x}, \triangle \dot{\mathbf{x}}, t) \leq \overline{C}_{ijk}^1 \triangle x_j \triangle x_k + \overline{C}_{ijk}^2 \triangle x_j \triangle \dot{x}_k \tag{4.14}$$

is valid. From (4.8) follows:

$$\triangle \dot{x}_i = \frac{\partial}{\partial x_j} \widetilde{f}_i(\overline{\mathbf{x}}, t) \triangle x_j + \frac{\partial^2}{\partial x_j \partial x_k} \widetilde{f}_i(\xi, t) \triangle x_j \triangle x_k \quad \xi \in [0, \triangle \mathbf{x}]$$

where $\widetilde{\mathbf{f}} = \mathbf{M}^{-1}\mathbf{f}$. Hence from (4.14) follows, that within Q

$$m_{ij}^{-1}(t)h_j(\triangle\mathbf{x}, \triangle\dot{\mathbf{x}}, t) \leq \overline{C}^1_{ijk}\triangle x_j \triangle x_k + \overline{C}^2_{ijk}\triangle x_j(\frac{\partial}{\partial x_l}\widetilde{f}_k(\overline{\mathbf{x}}, t)\triangle x_l + \frac{\partial^2}{\partial x_l \partial x_m}\widetilde{f}_k(\xi, t)\triangle x_l \triangle x_m), \qquad \xi \in [0, \triangle\mathbf{x}]$$

holds and hence

$$m_{ij}^{-1}(t)h_j(\triangle\mathbf{x}, \triangle\dot{\mathbf{x}}, t) \leq \overline{C}^3_{ijk}\triangle x_j \triangle x_k . \tag{4.15}$$

The right hand side of (4.15) is of order 2 and $m_{ij}^{-1}(t)h_j(\triangle\mathbf{x} = 0, \triangle\dot{\mathbf{x}}, t) = 0$. Hence it has been shown that there exists a domain $\|\triangle\mathbf{x}\|_\infty < H$ where (4.10) is valid. Therefore stability for the system of the type $\mathbf{M}\dot{\mathbf{x}} = \mathbf{f}$ can also be determined by the first approximation.

Eigenvalues of the Monodromy Matrix

We now calculate the monodromy matrix corresponding to (4.9). One integrates $\mathbf{M}(t)\triangle\dot{\mathbf{x}} = \mathbf{A}(t)\triangle\mathbf{x}$ over one period T with linearly independent initial conditions. The columns of the monodromy matrix $\mathbf{B}$ consist of the solution vectors calculated with the different initial conditions

$$\mathbf{B} = [\mathbf{x}(T, \mathbf{x}_0 = \mathbf{e}_1), ..., \mathbf{x}(T, \mathbf{x}_0 = \mathbf{e}_6)] ,$$

with $\mathbf{e}_1 = [1, 0, 0, 0, 0, 0]^T$, $\mathbf{e}_2 = [0, 1, 0, 0, 0, 0]^T, ...$ For the given set of parameters (cf. Appendix A) the eigenvalues of the monodromy matrix $\mathbf{B}$ are given in Table 3. One sees

Table 3. Eigenvalues of $\mathbf{B}$ (3 DOF motor model)

eigenvalue	value	absolute value
λ_1, λ_2	-0.7101 ± 0.5908i	0.9238
λ_3	0.8416	0.8416
λ_4	0.8272	0.8272
λ_5, λ_6	-0.6570 ± 0.0189i	0.6573

that as shown in Fig. 12 all eigenvalues of the monodromy have an absolute value which is less than 1. Hence the steady state solution for the given set of parameters is stable in the sense of LIAPUNOV.

Parameter variations show that if a steady state solution exists this solution is always stable, [5].

5. EXTENSION OF THE MODEL

According to the assumptions the case of slip between rotor and stator has not been included so far. As a consequence with a sufficiently large excitation torque it was always possible to drive the rotor for any arbitrary loading torque T. The restrictions of the contact condition $F_t \leq \mu F_n$ had to be checked separately. This can be improved by a modified contact condition.

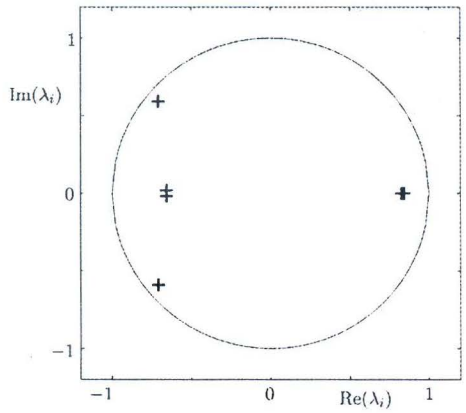

Fig. 12. Eigenvalues of the monodromy matrix for the set of parameters given in Appendix A

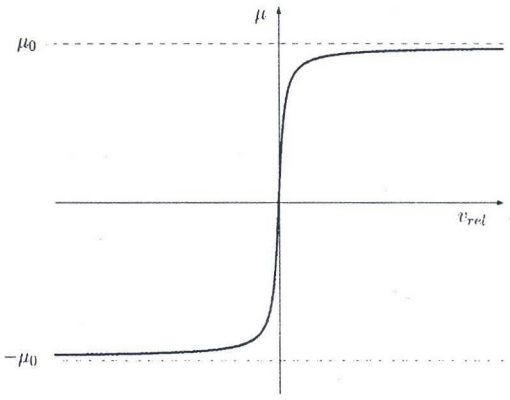

Fig. 13. Friction characteristic

Formulating the contact condition allowing slip

In order to allow slip in the model an additional degree of freedom has to be created. When slip occurs the angular velocity of the rotor is no longer coupled to the variables of the stator. Avoiding to switch between one model with 3 DOF and one with 4 DOF, the driving force for the rotor is described by

$$\begin{aligned} F_t &= \mu(v_{rel}) F_n \,, \\ v_{rel} &= v_c - \omega_R R^* \,, \quad \text{with} \quad v_c = (\vec{\omega} \times \vec{r}_c) \cdot \vec{e}_{x_1} \,. \end{aligned} \tag{5.1}$$

The characteristic $\mu(v_{rel})$ is given in Fig. 13. Analytically the characteristic of Fig. 13 is given by

$$\mu = \mu_0 \arctan(\kappa v_{rel}) \,. \tag{5.2}$$

The parameter μ_0 determines the maximum of μ, κ is the parameter for the slope of the curve. Again, we assume that there is contact between rotor and stator at any time. Hence, (2.3) remains valid.

Consequences for the equations of motion

Due to the new contact condition (5.1) the model now has an additional DOF, namely ϕ_R. The kinematic constraint (2.4) is no longer valid since slip between rotor and stator is possible. The new equations of motion are derived by substituting (5.1) into the equations (2.2) and (2.6). The equations of motion can again be written as a first order system

$$\mathbf{M}(\mathbf{x})\dot{\mathbf{x}} = \mathbf{f}(\mathbf{x}, t) \,, \tag{5.3}$$

where $\mathbf{M}$ is a 8×8 matrix and $\mathbf{f}(\mathbf{x}, t)$ is a 8×1 vector. The vector $\mathbf{x}$ is given by

$$\mathbf{x} = [\phi_R, \phi, \theta, \psi, \dot{\phi}_R, \dot{\phi}, \dot{\theta}, \dot{\psi}]^T \,.$$

Table 4. Eigenvalues of **B** (4 DOF motor model)

eigenvalue	value	absolute value
λ_1, λ_2	$0.2616 \pm 0.4934i$	0.5585
λ_3	0.7702	0.7702
λ_4	0.8269	0.8269
λ_5, λ_6	$-0.8021 \pm 0.2712i$	0.8467
λ_7	0.8654	0.8654
λ_8	1	1

Analysis of the stationary solution

The stationary solution of (5.3) is derived analogously as described in Section 3. The state vector takes the form

$$\bar{\mathbf{x}} = \left[\dot{\bar{\phi}}_R\, t, \Omega t + \alpha, \bar{\theta}, -\frac{\Omega t}{\cos\bar{\theta}} + \beta, \dot{\bar{\phi}}_R, \Omega, 0, -\frac{\Omega}{\cos\bar{\theta}}\right],$$

where $\dot{\bar{\phi}}_R = \text{const}$. The system of equations is then analogously formulated to the case of stick, with the unknowns $\dot{\bar{\phi}}_R, \bar{\theta}, \alpha, \beta$. For the given set of parameters and $\mu_0 = 0.3$, $\kappa = 20$ one obtains $\dot{\bar{\phi}} = -10.34$ 1/s, $\theta = 0.81836 \cdot 10^{-4}$, $\alpha = 5.12$ and $\beta = -5.12$.

Stability analysis of the extended model

Stability analysis is performed as described in Section 4. Substituting the steady state solution into (5.3) and expanding about $\bar{\mathbf{x}}$ yields a linear system of equations with periodic coefficients. As in stability investigations for the model having 3 DOFs the FLOQUET theory is applied here analogously. For the given set of parameters (Appendix A) and $\mu_0 = 0.3$, $\kappa = 20$ one obtains the eigenvalues presented in Fig. 14 and listed in Table 4. Note $|\lambda_8| = 1$ which is due to a cyclic variable. Since the absolute value of all other

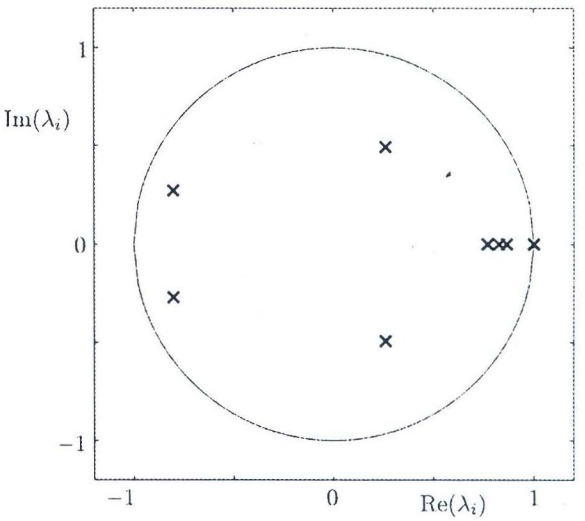

Fig. 14. Eigenvalues of the monodromy matrix for model with 4 DOF

eigenvalues are < 1 the solution for the given set of parameters is also stable in the sense of LIAPUNOV.

For both models (3 and 4 dof) stability investigations including parameter variations for m_0, Ω, and T have been performed, [5]. In both cases the steady state solution is always stable if the solution for the given set of parameters exists.

6. CONCLUSION

In this paper we introduced a simple mathematical model of a wobbling disk USM. In particular the stationary behavior of the motor and its stability were investigated in detail. The model offers insight in dynamic phenomena and identifies crucial motor parameters which influence the performance of the motor. The reduction in speed between the rotational speed of the rotor and the excitation frequency is of the order of magnitude $\approx 10^4$, ..., which accounts for one of the advantages of piezoelectric traveling wave motors. While the excitation frequency influences the rotor speed directly, other parameters such as the excitation amplitude and the loading torque vary and control the rotor speed indirectly via the tilting angle. The stability analysis proves that the steady state solution is robust against small disturbances.

Only few motor models, adequate for motor design and optimization, exist today. Motor developments done through experimental efforts indicate long procedures and often times do not provide a deeper insight into the mechanisms. An advanced understanding of the USM, which is provided by analytical studies, is precious in the sense of reducing such experimental efforts. Problems such as e.g. the occurrence of parasitic vibrations which often result in an unsteady operation or the appearance of squealing in the early stage of motor design can not only be analyzed with such a mathematical background but also their origin may be identified. Due to the complexity and computational expenses of piezoelectric motors in general a simple mathematical model such as presented in this paper enhances the optimization process by providing detailed understanding of the dynamical behavior of such a motor.

A. PARAMETERS

Table 5. Motor parameters

parameter	value	unit
m_0	0.005	Nm
T	$6.46 \cdot 10^{-5}$	Nm
F_0	0.4	N
c_R	4000	N/m
d_R	0.1632	Ns/m
c_t	10000	Nm
c_r	924.6677	Nm
d_t	$9.1232 \cdot 10^{-4}$	Nms
d_r	$2.3865 \cdot 10^{-4}$	Nms
R	0.005	m
H	0.003	m
I_R	$7.9522 \cdot 10^{-9}$	kgm^2
I_{xx}	$1.7109 \cdot 10^{-8}$	kgm^2
I_{yy}	$1.7109 \cdot 10^{-8}$	kgm^2
I_{zz}	$2.3120 \cdot 10^{-8}$	kgm^2

REFERENCES

1. T. R. Sattel, Dynamics of Ultrasonic Motors, *Ph. D. Thesis*, Technische Universitt Darmstadt, 2002.
2. M. Berg, Ein Wanderwellenmotor mit zylindrischem Stator: Mathematische Modellierung und experimentelle Unetersuchungen, *Ph. D. Thesis*, Technische Universitt Darmstadt, 2001.
3. I. Okumura, A designing method of a bar-type ultrasonic motor for autofocus lenses, *IFToMM-jo International Symposium on Theory of Machines and Mechanisms*, 1992.
4. S. Gutschmidt, *Mathematical-mechanical modeling of wobbling disk piezoelectric motors*, *Ph. D. Thesis*, Technische Universitt Darmstadt, 2005.
5. G. Spelsberg-Korspeter, Stabilittsberechnungen an einem Ultraschallmotor, *Master's Thesis*, Technische Universitt Darmstadt, 2004.
6. P. Hagedorn, *Non-Linear Oscillations*, Calendon Press Oxford, 1988.
7. J. G. Malkin, *Theorie der Stabilitt einer Bewegung*, R. Oldenburg, 1959.

Received June 5, 2007.

MÔ HÌNH HOÁ VÀ PHÂN TÍCH ỔN ĐỊNH ĐỘNG CƠ SIÊU ÂM

Việc phát triển các mô hình động cơ phù hợp với quá trình thiết kế và tối ưu hãy còn chưa đáp ứng được tình trạng kỹ thuật hiện nay. Lý do là trong mấy năm trước đây người ta thường nhấn mạnh tới việc tìm kiếm các nguyên lý hay chế tạo kiểu mẫu mới cho động cơ siêu âm trong khi hiện nay đã đòi hỏi phải tối ưu hoá hệ thống động cơ. Bài báo trình bày việc mô hình hoá động cơ piezoelectric dạng đĩa rung. Đã xây dựng lời giải bình ổn và nghiên cứu ổn định. Điều này cho phép hiểu biết sâu sắc bản chất của các quá trình động lực học của động cơ. Các kết quả có thể giúp định hướng trong việc hiểu biết nguyên lý làm việc, động lực học, đánh giá các tham số liên quan đến độ tin cậy, hoạt động ổn định và tối ưu hoá các loại động cơ trên.